Suppression of resistive wall instabilities with distributed, independently controlled, active feedback coils

C. Cates, M. Shilov, M. E. Mauel,[a] G. A. Navratil, D. Maurer, S. Mukherjee, D. Nadle, J. Bialek, and A. Boozer
Department of Applied Physics and Applied Mathematics, Columbia University, New York, New York 10027

(Received 11 February 2000; accepted 4 May 2000)

External kink instabilities are suppressed in a tokamak experiment by either (1) energizing a distributed array of independently controlled active feedback coils mounted outside a segmented resistive wall or (2) inserting a second segmented wall having much higher electrical conductivity. When the active feedback coils are off and the highly conducting wall is withdrawn, kink instabilities excited by plasma current gradients grow at a rate comparable to the magnetic diffusion rate of the resistive wall. © *2000 American Institute of Physics.* [S1070-664X(00)02308-9]

Conducting walls placed near toroidal plasmas such as those created in tokamaks,[1] reversed field pinches (RFP),[2] and spherical tori[3] can prevent or reduce the growth of harmful, long-wavelength MHD (magnetohydrodynamic) instabilities. For this reason, many attractive fusion power scenarios require wall stabilization to reach high fusion power density and operate continuously with low recirculating power.[13–15] Long-wavelength modes are stabilized by close fitting conducting walls because wall eddy currents oppose the helical perturbations created by these instabilities. Passive wall stabilization can fail when the eddy currents decay due to the finite resistivity of the wall, allowing resistive wall modes (RWM) to grow on the time scale of magnetic diffusion through the wall, τ_w.[4,5] RWMs have been identified in RFPs[6,7] and in tokamaks.[8–10] In RFP experiments, both the lifetime of the discharge and the growth time of the RWM were observed to increase as τ_w increased. In tokamak discharges, the relationship between wall position and wall stability was demonstrated by moving an adjustable conducting wall near the plasma edge which stabilized fast growing external kink instabilities and delayed disruptions.[11] Additionally, the wall eddy currents induced by external kink instabilities have been measured in detail and found to resemble ideal MHD calculations.[12]

Although wall-stabilized plasmas have been produced transiently which satisfy the requirements for attractive high-beta steady-state tokamak operation,[16] a present challenge is to maintain the effectiveness of wall stabilization for very long times relative to τ_w. Three schemes have been proposed: The plasma can be rotated with respect to the walls,[17–21] a nearby, secondary wall can be rotated with respect to the plasma,[22] or a network of active feedback coils can be configured so as to simulate a perfectly conducting wall[23,24] or a ''fake'' rotating wall.[25] Although the rate of toroidal rotation needed to stabilize the RWM is seen experimentally to be lower than originally expected,[26] active feedback is an important approach to RWM control since the physical mechanisms producing RWM stability with rotation are still unknown[27] and toroidal coupling to poloidal sidebands which resonate with magnetic surfaces within the plasma may act to break the plasma's rotation at high beta.[28]

Previous magnetic feedback experiments used a small number of feedback circuits to interact with a single toroidal and poloidal mode.[6,29,30] In this Letter, we report the first use of a distributed network of independently controlled active feedback coils to suppress the growth of current-driven resistive wall modes. Although the RWMs were observed to rotate, this rotation did not prevent the growth of resistive wall modes. The results from these experiments support the feasibility of sustained wall stabilization through the use of active feedback coils.

The experiments were carried out using the HBT-EP tokamak which previously demonstrated passive wall stabilization of external kink modes by adjusting the position of a segmented aluminum (Al) wall.[11] Each wall segment can be independently positioned $(1.08<b/a<1.70)$, allowing the position of the wall to be adjusted relative to the plasma. Half of the original thick (1.2 cm) Al wall segments were replaced with thinner (0.2 cm) stainless steel (SS) segments at equally spaced toroidal locations. The active feedback system is illustrated in Fig. 1 and consists of thirty flux loop sensors and thirty control coils mounted to the SS wall segments on the side not facing the plasma. At each of the five equally spaced toroidal locations there are two SS segments, top and bottom. There are three, overlapping, 15-turn control coils on each segment with a poloidal angular width of $\sim 55°$ and spaced 25° apart. Each SS wall segment also has three 20-turn sensor loops in the center of its corresponding control coil. The areas of the sensor loops are slightly less than half the area of the control coils in order to reduce their mutual inductance.

For toroidally continuous walls, the characteristic time for magnetic diffusion is given by $\tau_w=\mu_0 b d/\rho$, where b is the minor radius of the wall, d is the wall thickness, and ρ is the resistivity. For the HBT-EP wall, these times are equal to 65 and 0.4 ms, respectively, for Al and SS. For segmented walls, the RWM will still grow at a rate inversely proportional to wall time, $1/\tau_w$; however, the segmented wall must be moved closer to the plasma than for a complete wall to stabilize the fast ideal mode.[31] Wall stabilization observed for many positions of the HBT-EP segmented wall are consistent with this prediction.[32] For the experiments reported here, the SS wall segments were always fully inserted, and the Al wall segments were either fully inserted or fully re-

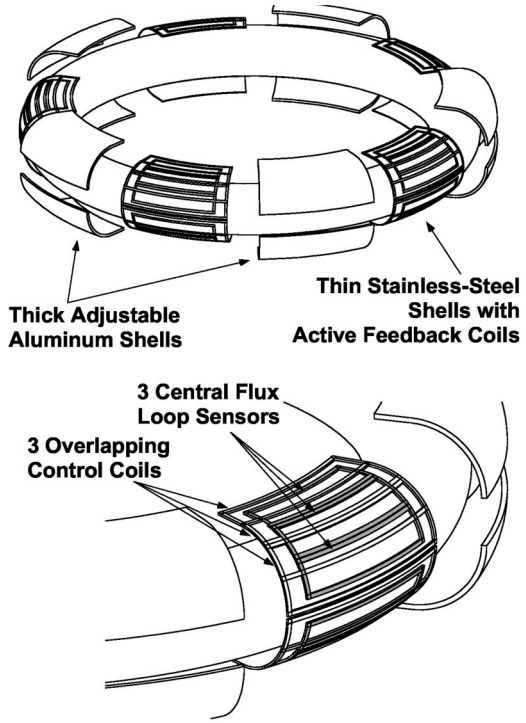

FIG. 1. HBT-EP's adjustable conducting wall consists of ten Al segments and ten SS segments. Flux sensors and control coils are mounted onto the SS segments. Each conducting shell can be independently positioned with respect to the plasma.

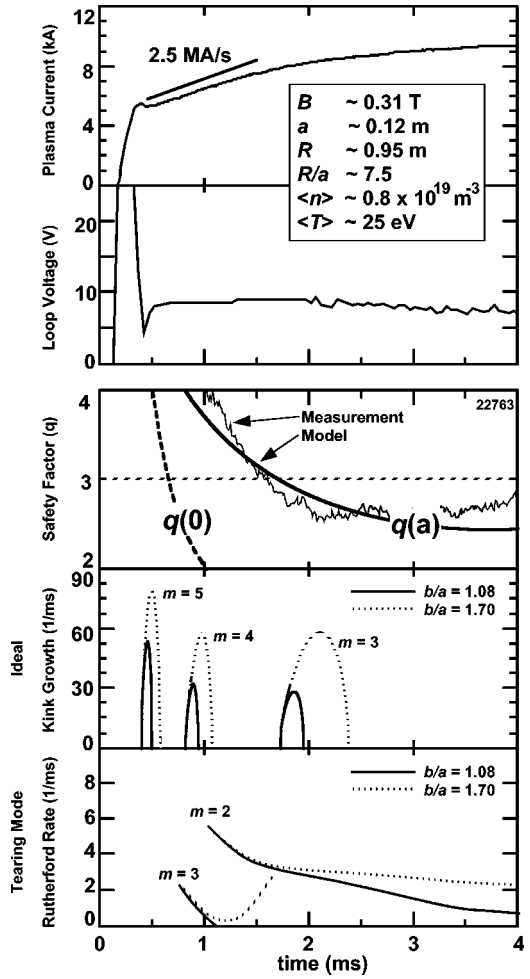

FIG. 2. Time evolution of a ''current ramp'' discharge which is unstable to current-driven kink instabilities and tearing modes. By using a one-dimensional (1D) transport code, experimental measurements can be approximately reproduced, and the instability growth rates can be calculated from the evolving current-profile as a function of wall position.

tracted. When the Al wall segments were inserted, passive wall stabilization occurred. When the Al wall segments were fully retracted, the RWM was excited reproducibly which allowed study of active RWM feedback stabilization.

Each sensor loop and control coil pair of the active feedback system was connected to an identical and independent feedback circuit containing solid-state amplifiers and analog filters. Each feedback circuit produced a voltage proportional to both the flux, Φ_s, and the time-derivative of the flux, $\dot{\Phi}_s$, detected by a sensor. Near the center of the control system's bandwidth, 4 kHz, the control voltage was $V_c = G_d \dot{\Phi}_s + G_p \Phi_s$, with $G_d = 31$ V/V and $G_p = 5.5 \times 10^5$ V/Weber. Referring to the formulations of Okabayashi and co-authors,[33] the HBT-EP active feedback system resembles ''total flux feedback'' with a dimensionless gain between 4 and 6 and excludes up to 85% of the penetration of magnetic flux through the SS wall segments for magnetic fields up to 10 G within a bandwidth of 0.4 kHz$<\omega/2\pi<$11 kHz. For typical plasma experiments, the average radial magnetic field applied by the control coils was approximately one Gauss.

In the HBT-EP tokamak, plasma discharges are created using a fast-startup technique.[34] A large initial toroidal loop voltage, 150–500 V, ionizes the plasma and allows an initial penetration of plasma current to the plasma core. The temporal programming of the plasma current which occurs after the initial startup changes the characteristics of the MHD instabilities appearing later.[11] Pressure-driven external kinks with a global radial structure are excited when the initial plasma current is sufficiently large to increase the central ohmic heating rate and plasma temperature.[11,12] When the initial plasma current is lower, it is possible to apply a second, sustained current ramp which broadens the plasma current profile and excites edge-localized, current-driven external kink instabilities.

Discharges of the second type, called ''current-ramp discharges,'' are used for the experiments described here. Figure 2 shows the time evolution of the plasma current, loop voltage, and safety factor. The initial current ramp to 5 kA ionizes the plasma. The second current ramp to 9 kA generates a broad current profile. The plasma line-averaged density does not change significantly during the current ramp, and the plasma beta, $<0.2\%$, and poloidal beta, ~ 1, remain low.

For these discharges, the properties of MHD instabilities are determined from the current profile. Although the current profile could not be measured, a useful estimate of the current profile evolution was made by using a one-dimensional transport code.[34] The transport simulation was based on several assumptions: (1) the effective ion charge state, Z_{eff}, is near unity, (2) the ion and electron temperatures are equal, (3) the initial electron temperature and current profiles are uniform, (4) the plasma thermal diffusivity, χ_E, is uniform

and constant in time, and (5) the edge plasma temperature is constant in time. Measurements made in other similar discharges with a central Thomson scattering diagnostic and with movable magnetic and Langmuir probes are consistent with these assumptions. For the discharge shown in Fig. 2, the transport simulation reproduces the measured loop voltage when the edge temperature is 5 eV and $\chi_E = 9\ \mathrm{m}^2/\mathrm{s}$. As the current increases, the central safety factor, $q(0)$ decreases from 5 and reaches 1 at ~3 ms. Except for the first few hundred μs, the current density monotonically decreases with minor radius.

Since the HBT-EP plasmas have a large aspect ratio, $R/a \sim 7.5$, the long-wavelength MHD stability of these low-pressure plasmas can be computed using a cylindrical treatment.[36] Both external kink modes and tearing modes are found to be unstable. Figure 2 shows the growth rates for the ideal $n=1$ external kink and the resistive $n=1$ tearing mode. The illustrated growth rates correspond to the case when the plasma is surrounded by a perfectly conducting cylindrical wall at the two positions studied experimentally, $b/a = 1.08$ and 1.70. External kink instabilities are expected to appear for brief transient intervals, only fractions of a millisecond long, shortly after $q(a)$ decreases below an integral value. The growth rates of the external kinks are strongly influenced by wall position. Tearing modes are unstable throughout the discharge, but they grow more slowly than kink modes. Wall position also reduces the growth of tearing modes, but stabilization only occurs when the rational surface approaches the edge of the plasma. These edge tearing modes are sometimes called ''resistive kink modes.''[36]

MHD fluctuations which coincide with the expected appearance of instability are detected by the sensor loops of the active feedback system and by a poloidal array of Mirnov coils mounted on the inside of an Al wall segment. The voltages from five sensor loops located at the same poloidal angle and equally spaced toroidally are used to compute the magnitude of the nonaxisymmetric, $n=1$, rate of flux penetration through SS wall segments. The poloidal Mirnov coils are used to monitor the size and poloidal structure of the magnetic perturbations.

Figure 3 shows the effects of passive wall stabilization and of active feedback control on the magnetic fluctuations. The figure shows three typical plasma discharges which are nearly identical except for the arrangement and use of the adjustable wall segments. Discharge number 22 763 had the Al wall segments fully inserted, $b/a = 1.07$. The other two discharges (numbered 22 780 and 22 781) had the Al segments fully retracted, $b/a = 1.70$. When the Al wall was inserted, a short burst of $n=1$ activity was observed on the sensor loops as $q(a)$ approached and passed below 3. This was accompanied by an equally short burst of Mirnov oscillations. Approximately 0.5 ms later, $m=2$ tearing modes saturated with a relatively large amplitude, $\delta B_\theta / B_\theta(a) \sim 5\%$. The tearing modes rotate near the electron diamagnetic drift frequency, ≈ 10 kHz, and these modes have been described in detail elsewhere.[30]

When the Al segments are retracted and the active feedback control is off (22 780), the amplitude of the $m=3$ oscillations increase significantly when $q(a) \sim 3$. The poloidal

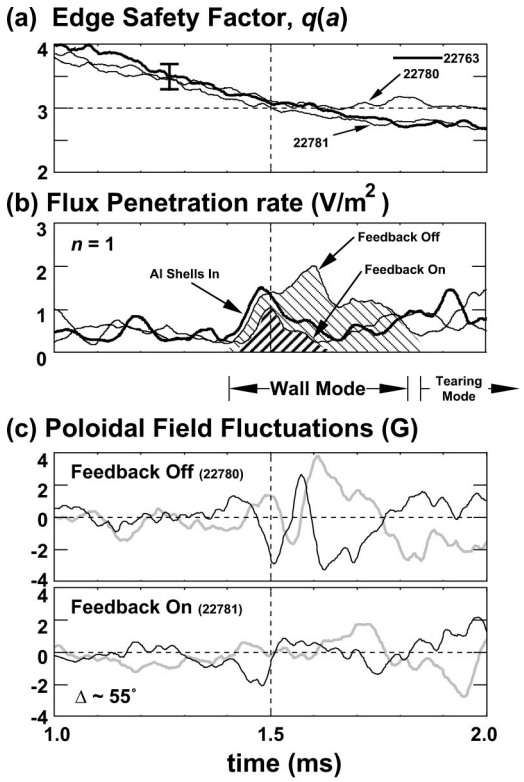

FIG. 3. Three similar discharges illustrate stabilization of the ($m=3$, $n=1$) edge kink instability by either inserting the thick Al wall segments or by switching on active feedback control. The figure shows (a) the edge safety factor, (b) the rate of non-axisymmetric ($n=1$) flux penetration through the SS wall, and (c) the perturbed poloidal field from two Mirnov coils separated poloidally by 55°.

field perturbations, δB_θ, increase at a rate as large as $15 \times 10^3\ \mathrm{s}^{-1}$ and clearly show a poloidal structure of an external mode. Perturbed $n=1$ flux is driven through the SS wall for a period lasting 0.4 ms. This growth rate is much less than the ideal MHD growth rate with the wall retracted, and it is also 2 to 3 times faster than the expected growth rate of a resistive kink in the absence of a wall. The growing $m=3$ mode initially rotates near a frequency between 5 kHz $< \Omega/2\pi < 7$ kHz. The rotation rate slows after reaching peak amplitude. This time also coincides with the onset of a minor disruption and a 1 cm decrease in the plasma major radius. The discharge eventually recovers, and saturated $m=2$ tearing modes appear for $t > 3$ ms. This behavior is typical of other HBT-EP discharges that do not terminate with a major disruption during the current ramp[11] and that have plasma lifetimes (a measure of ''performance'') dependent on the saturated levels of tearing modes during the current flat-top. For the plasmas described here, the short RWM bursts neither caused major disruptions nor influenced tearing mode amplitude, and, as a consequence, overall discharge lifetime was not influenced by Al shell position (or with the application of feedback).

When the active feedback control is switched on (22 781), the amplitudes of the $m=3$ fluctuations and $n=1$ flux penetration rate decrease to levels at or below those observed when the Al segments are fully inserted. Similar levels of growth rate suppression were reproduced on ten

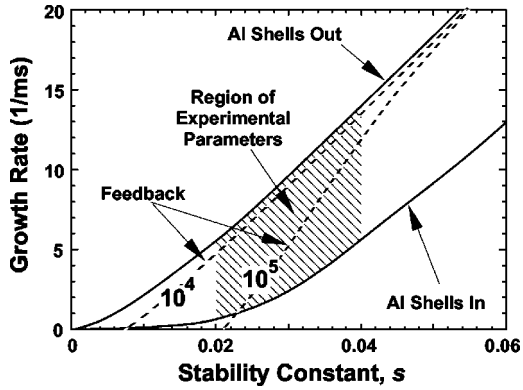

FIG. 4. The instability growth rate computed for the actual HBT-EP segmented wall and active control system using a 3D electromagnetic code and the technique described by Boozer (Ref. 35). The cross-hatched region indicates parameters consistent with experimental observations. The SS segments are always inserted, but the growth rate of the RWM is significantly decreased by insertion of the Al wall segments. With the Al segments retracted but with active feedback on, a similar reduction of RWM growth rates can occur when the gain of the active feedback system exceeds 10^5 V/Weber.

discharges prepared in the same way as 22 781. At the present time, the only difference consistently detected between the MHD behaviors of discharges stabilized with Al wall segments or with active feedback is the earlier onset of tearing mode rotation occurring with feedback.

The growth rate of the $n=1$ mode seen without feedback (22 780) corresponds to expectations for the RWM (approximately $2m/\tau_w$ in the cylindrical limit). Using a variational technique,[37] the RWM growth rate calculated with a cylindrical approximation peaks at $20\times10^3\,\mathrm{s}^{-1}$ and decreases quickly as $q(a)$ decreases in time.

The RWM growth rate, with and without active feedback, can also be calculated with accurate wall and control coil geometry using the technique developed by Boozer[35] and a (3D) three-dimensional, finite element, electromagnetic computer code such as the VALEN code being developed by Bialek.[38] In Boozer's prescription, wall instability is parameterized in terms of a dimensionless stability constant, $s\propto-\delta W/\tilde{\Phi}^2$, where δW is the change in plasma energy and $\tilde{\Phi}$ is the perturbed magnetic flux due to the MHD perturbation. Instability occurs when $s>0$ for any wall with finite τ_w, and increasing s corresponds to stronger instability drive. Figure 4 summarizes the computed growth rates of the external mode when $q(a)<3$ for the HBT-EP wall and coil geometries. A region coinciding with the parameters observed in the experiment is indicated by cross-hatching. When $0.02<s<0.04$, the effect of moving the Al wall segments (while keeping the SS segments near the plasma) is change the RWM growth rate as seen experimentally. When retracted, the RWM growth rate is near $10^4\,\mathrm{s}^{-1}$, and, when inserted, the growth rate is reduced sufficiently as to make detection difficult. Within this region, the calculations also indicate that feedback can be effective provided the effective gain is greater than about 10^5 V/Weber, consistent with the experimental observations.

In summary, the growth of RWMs has been suppressed by energizing a network of active feedback control coils. The observed stabilization resembles passive wall stabilization achieved by moving a highly conducting wall to the edge of the plasma and is consistent with 3D electromagnetic calculations. Further details of these and additional investigations of the active control of RWMs will be reported in a separate article. Investigations now underway include the study of high-beta discharges, improved q profile measurements, and optimization of the active feedback circuits.

This work has been supported by U.S. Department of Energy Grant No. DE-FG02-86ER53222. The authors gratefully acknowledge the help from R. Fitzpatrick, T. H. Jensen, and N. Rivera during the design and construction of the HBT-EP active feedback system.

[a]Electronic mail: mauel@columbia.edu

[1]E. J. Strait, Phys. Plasmas **1**, 1415 (1994).
[2]H. A. B. Bodin, Nucl. Fusion **30**, 1717 (1990).
[3]T. C. Hender, S. J. Allfrey, R. Akers *et al.*, Phys. Plasmas **6**, 1958 (1999).
[4]D. Pfirsch and H. Tasso, Nucl. Fusion **11**, 259 (1971).
[5]C. G. Gimblett, Nucl. Fusion **26**, 617 (1986).
[6]B. Alper, Phys. Fluids B **2**, 1338 (1990).
[7]P. Greene and S. Robertson, Phys. Fluids B **5**, 556 (1993).
[8]E. J. Strait, T. S. Taylor, A. D. Turnbull *et al.*, Phys. Rev. Lett. **74**, 2483 (1995).
[9]A. M. Garofalo, A. D. Turnbull, M. E. Austin *et al.*, Phys. Rev. Lett. **82**, 3811 (1999).
[10]M. Okabayshi, N. Pomprey, J. Manickam *et al.*, Nucl. Fusion **36**, 1167 (1996).
[11]T. H. Ivers, E. Eisner, A. Garafalo *et al.*, Phys. Plasmas **3**, 1926 (1996).
[12]A. M. Garofalo, E. Eisner, T. H. Ivers *et al.*, Nucl. Fusion **38**, 1029 (1998).
[13]A. D. Turnbull, T. S. Taylor, Y. R. Lin-Liu, and H. St. John, Phys. Rev. Lett. **74**, 718 (1995).
[14]C. Kessel, J. Manickam, G. Rewoldt, and T. M. Tang, Phys. Rev. Lett. **72**, 1212 (1994).
[15]R. L. Miller, Y. R. Lin-Liu, A. D. Turnbull, Y. S. Chan, L. D. Pearlstein, O. Sauter, and L. Villard, Phys. Plasmas **4**, 1062 (1997).
[16]E. J. Strait, L. L. Lao, M. E. Mauel *et al.*, Phys. Rev. Lett. **75**, 4421 (1995).
[17]T. H. Jensen and M. S. Chu, J. Plasma Phys. **30**, 57 (1983).
[18]A. Bondeson and D. J. Ward, Phys. Rev. Lett. **72**, 2709 (1994).
[19]M. S. Chu, J. M. Greene, T. H. Jensen, R. L. Miller, A. Bondeson, R. W. Johnson, and M. E. Mauel, Phys. Plasmas **2**, 2236 (1995).
[20]R. Betti and J. P. Freidberg, Phys. Rev. Lett. **74**, 2049 (1995).
[21]A. Boozer, Phys. Plasmas **2**, 4521 (1995); **3**, 4620 (1996).
[22]C. G. Gimblett, Plasma Phys. Controlled Fusion **31**, 2183 (1989).
[23]C. M. Bishop, Plasma Phys. Controlled Fusion **31**, 1179 (1989).
[24]T. H. Jensen and R. Fitzpatrick, Phys. Plasmas **4**, 2997 (1997).
[25]R. Fitzpatrick and T. H. Jensen, Phys. Plasmas **3**, 2641 (1996).
[26]T. S. Taylor, E. J. Strait, L. L. Lao *et al.*, Phys. Plasmas **2**, 2390 (1995).
[27]A. M. Garofalo, A. D. Turnbull, E. J. Strait *et al.*, Phys. Plasmas **6**, 1893 (1999).
[28]C. G. Gimblett and R. J. Hastie, Phys. Plasmas **7**, 258 (2000).
[29]A. W. Morris, T. C. Hender, J. Hugill *et al.*, Nucl. Fusion **32**, 2091 (1992).
[30]G. A. Navratil, C. Cates, M. E. Mauel, D. Maurer, D. Nadle, E. Taylor, and Q. Xiao, Phys. Plasmas **5**, 1855 (1998).
[31]R. Fitzpatrick, Phys. Plasmas **1**, 2931 (1994).
[32]E. Eisner, *The Effects of Wall Coverage, Symmetry, and Plasma-Wall Separation on the Stability of Tokamak Plasmas*, Ph.D. thesis, Columbia University (1998).
[33]M. Okabayashi, N. Pomprey, and R. E. Hatcher, Nucl. Fusion **38**, 1607 (1998).
[34]M. K. V. Sankar, E. Eisner, A. Garofalo *et al.*, J. Fusion Energy **12**, 303 (1993).
[35]A. Boozer, Phys. Plasmas **5**, 3350 (1998).
[36]J. A. Wesson, Nucl. Fusion **18**, 87 (1978).
[37]S. W. Haney and J. P. Friedberg, Phys. Fluids B **1**, 1637 (1989).
[38]J. Bialek, A. Boozer, M. Mauel, and G. Navratil, Bull. Am. Phys. Soc. **43**, 1831 (1998).